Tampere University

Robert Cantaragiu

NANOSTRUCTURING MULTILAYER HYPERBOLIC METAMATERIALS FOR ENHANCED EMISSION

Bachelor of Science Thesis
Faculty of Natural Sciences
Examiners: Assoc. Prof. Humeyra Caglayan
Mohsin Habib
May 2020

ABSTRACT

Robert Cantaragiu: Nanostructuring Multilayer Hyperbolic Metamaterials for Enhanced Emission
Bachelor of Science Thesis
Tampere University
Degree Programme
May 2020

Strong coupling of nano-antenna with the quantum emitters is required for many quantum applications. However, conventional plasmonic antenna suffer high losses due to spectral overlap of scattering and absorption. Previous studies have shown that scattering is the dominating electromagnetic decay channel and that hyperbolic metamaterial cavities have useful properties such as ultrasmall mode volumes and artificially engineered refractive indices which enable the enhancement of light-matter interactions at nanoscale. In this work, I have introduced Ag/SiO_2 alternating layers based hyperbolic meta-antennas as a potential candidate for separating the spectral overlap of absorption and scattering. I have numerically calculated the absorption and scattering of Ag/SiO_2 nano-antenna using finite difference time domain (FDTD) method. The interaction between the dye and the nanostructure depends on the shape, size and material used. Therefore the meta-antennas are designed to match the emission peak of LDS dye. Then, the hyperbolic-meta-antenna is fabricated on top glass substrate to study their coupling with LDS 750 dye. I experimentally demonstrate that the scattering overlap with the emission peak of the dyes and the separation of the absorption spectrum play a role in the emission enhancement of the dyes. The photoluminescence measurements show 1.5 enhancement of the emission of LDS dye on top hyperbolic meta-antenna. These meta-antenna can be used to design solid state light sources and quantum technologies.

Keywords: hyperbolic metamaterial, quantum emitter, nano-antenna, e-beam evaporator, spontaneous emission

PREFACE

Firstly, I would like to express my deepest gratitude towards Professor Humeyra Caglayan for guiding, supporting and helping me throughout my thesis and bachelor studies. From almost the beginning of my studies she taught me most of the things about nanophysics, simulation software and provided me with answers to every question I had regarding my thesis and work in the research group. Her leadership, team-building skills and enthusiasm made me feel very welcome and grateful to work in the Metaplasmonics group.

I am very thankful to Mohsin Habib for teaching me a lot about nanofabrication and training me how to use the devices from the cleanroom. He has been my mentor for almost a year now and always helped and supported me with everything I needed during my thesis and work in the research group. He also was reviewing my thesis and his comments were very helpful in regards to making this work. I am very grateful for working with him and for everything he taught me and helped me with.

I would also like to thank Dr. Alireza Rahimi Rashed for all the guidance he gave me during my work in the research group and for teaching me about nanocharacterization in the lab. He is a great teacher and the way he explains everything in much detail helps me have a deeper understanding of the topic at hand.

Finally I would like to thank all the members of the Metaplasmonics research group for helping me with all I needed and making me feel very grateful to for in this group.

Tampere, 31st May 2020

Robert Cantaragiu

CONTENTS

LIST OF FIGURES

LIST OF SYMBOLS AND ABBREVIATIONS

ϵ	Dielectric permittivity
γ	Decay rate
$\mathbf{F}$	Purcell factor
$\mathbf{P}$	Power
FDTD	Finite difference time domain
HMM	Hyperbolic metamaterials
LDOS	Local density of states
LSPR	Localized surface plasmon resonance
PL	Photoluminescence
PML	Perfectly matched layer
PMMA	Polymethyl methacrylate
QD	Quantum dots
RIE	Reactive ion etcher
SEM	Scanning electron microscope
TAU	Tampere University
TUNI	Tampere Universities
URL	Uniform Resource Locator

1 INTRODUCTION

Metamaterials are artificial materials composed of meta-atoms to exhibit artificial optical properties to manipulate light. Initially, the metamaterials were studied to obtain negative permittivity and negative permeability. The type of materials are known as double negative materials. The name meta comes from the fact that double negative materials are not available naturally. The hyperbolic metamaterial (HMM) is subclass of metamaterials. The HMM are alternating layers of metal and dielectric materials with hyperbolic dispersion surface in the momentum space, unlike the spherical or ellipsoidal dispersion of normal materials [1], [2]. This hyperbolic dispersion exhibits modifications in the local density of states (LDOS) around and inside the HMMs, which makes emitters placed near the HMMs have an enhancement in their emission [3]. Some fields where enhancing spontaneous emission from optical nanostructures that can couple to emitters is desirable include: quantum computing, optical communications, quantum information processing and fluorescence imaging [4].

The plasmonic nanoantenas can confine the light down to the nanoscale. They are used to manipulate light at the subwavelength level for energy harvesting, photovoltaics, lasing and biomedical sensing. The fundamental limitation of plasmonic nanostrucutres is that the localized surface plasmon resonances (LSPRs) of these antennas have overlapping scattering and absorption. It is important to have high scattering for guiding the light and high absorption in imaging applications. Scattering is the dominating electromagnetic decay channel, when an electric dipolar mode is induced in the system. A potential idea for enhancing the fluorescence emission is the coupling of nanostructures that have a spectral overlap of scattering with the emission of the quantum emitters. The plasmonic antenna limits the efficiency of both application due to the overlap. Therefore, as solution to this, one can design the nanoantenna in such a way that it can control/separate the absorption and scattering [5]. The hyperbolic meta-antennas (nanodisks composed of alternative metal and dielectric layer) were used for spectral distribution of the scattering and absorption.

This work focuses on using similar Ag/SiO_2 meta-antennas whose scattering peak overlaps with the emission peak of LDS 750 dyes to achieve emission enhancement.

2 BACKGROUND

2.1 Hyperbolic metamaterials

Hyperbolic metamaterials(HMMs) are metamaterials that use the concept of engineering the dispersion relation of waves to get unparalleled electromagnetic modes. Essentially, hyperbolic metamaterials act as polaritonic crystals where the coupled states of light and matter give rise to a larger density of electromagnetic states [6], [7]. The potential applications for these hyperbolic metamaterials would be negative refraction [8], [9], sub-diffraction imaging [10], sub-wavelength modes [11], and spontaneous emission [12] and thermal emission engineering [13], [1].

Light waves propagate uniformly in all orientations while they are in an isotropic medium such as vacuum. Their propagation can be thought as a spherical surface described by the equation $k_x^2 + k_y^2 + k_z^2 = \omega^2/c^2$. In this equation, $\vec{k} = [k_x, k_y, k_z]$ is the wavevector of the propagating wave, c is the speed of light in vacuum and ω represents the radiation frequency. In an uniaxial anisotropic medium the permittivity should also be taken into account and so the propagation of the wave is now described by the equation:

$$\frac{k_x^2 + k_y^2}{\epsilon_{zz}} + \frac{k_z^2}{\epsilon_{xx}} = \frac{\omega^2}{c^2}$$

Where ϵ is the permittivity of the medium and can be described by the following matrix:

$$\begin{bmatrix} \epsilon_{xx} & 0 & 0 \\ 0 & \epsilon_{yy} & 0 \\ 0 & 0 & \epsilon_{zz} \end{bmatrix}$$

In this uniaxial anisotropic medium, the permittivity components parallel to the electric field are $\epsilon_{xx} = \epsilon_{yy} = \epsilon_{\parallel}$ and the component perpendicular to the direction of propagation of light is $\epsilon_{zz} = \epsilon_{\perp}$. In an isotropic medium, the permittivity components are equal to each other $\epsilon_{xx} = \epsilon_{yy} = \epsilon_{zz}$ so the propagation shape of the wave is spherical. However, in an anisotropic medium $\epsilon_{xx} = \epsilon_{yy} \neq \epsilon_{zz}$ the shape becomes an ellipsoid and opens into a hyperboloid shape when the non-equal dielectric permittivity components are of opposite signs.

There are two types of hyperbolic metamaterials. In type I, only one component of the

permittivity is negative ($\epsilon_{xx} = \epsilon_{yy}$ >0, ϵ_{zz} < 0,) while in type II there are two negative components ($\epsilon_{xx} = \epsilon_{yy}$ < 0, ϵ_{zz} > 0). The two types along with the isotropic medium are represented in Figure 2.1. It should be noted that if all the permittivity components are positive the material would be a dielectric and if all the components are negative,the material is a metal. Type II HMMs are more reflective than Type I HMMs.

This work focuses on hyperbolic metamaterials made from alternating layers of Ag and SiO_2.

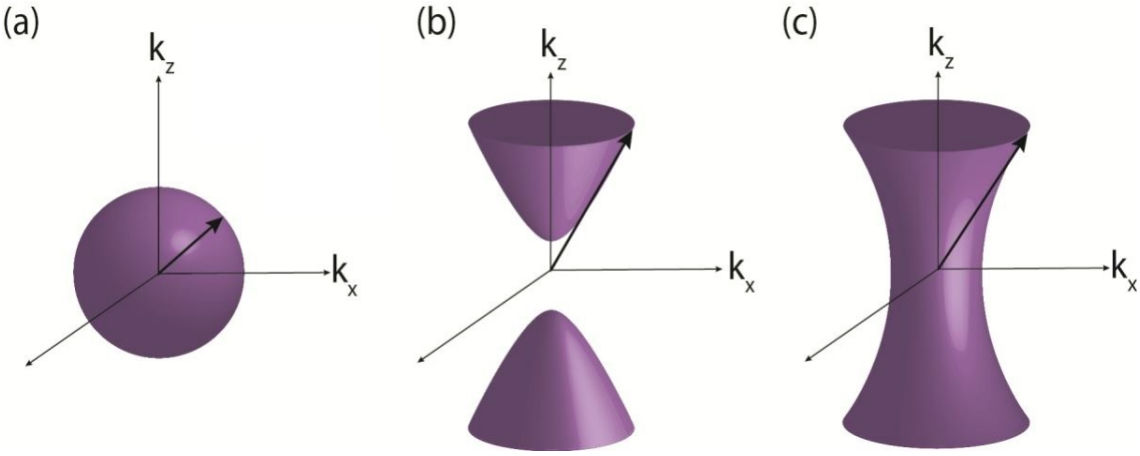

Figure 2.1. *(a) Wave propagation in an isotropic medium. (b) Hyperboloid propagation surface in Type I HMMs:* $\epsilon_{xx} = \epsilon_{yy}$ *> 0,* ϵ_{zz} *< 0 (c) Hyperboloid propagation surface in Type II HMM:* $\epsilon_{xx} = \epsilon_{yy}$ *< 0,* ϵ_{zz} *> 0. [1]*

2.2 Plasmonic nanoantennas

In the interaction between light and metal nanoparticles, the conduction electrons begin oscillating collectively. This phenomena is called localized surface plasmon resonances (LSPRs).

LSPRs enable an efficient way to transfer energy from the near-field to the far-field of the metal nanoparticles and vice versa. Therefore, one can call these nanostructures as nanoantennas, because they behave as a radio antenna would, at a higher frequency. Normally, these metalic nanoantennas are made from gold and silver due to their good conducting properties and low absorption [14].

LSPRs can couple to the light emitted by the quantum emitters that reside near the nanoantennas. The small mode volume of LSPRs increases the local density of states which changes the optical properties such as quantum efficiency and decay rate of these emitters. This coupling is dependent of the dielectric function of the medium and the shape, dimentions and material of the nanoantennas [14]. The coupling efficiency can be described by the absorption and scattering of the nanostructure.

Typically, in metallic nanoantennas, the scattering and absorption maximas overlap, which limits the full potential of the radiative decay of the emitters. The dominating electromagnetic decay is induced by the scattering and reduced by the absorption. To obtain a more

efficient decay channel, one must find a way to separate the spectral overlap of scattering and absorption and use quantum emitters whose emission has a spectral overlap with the scattering of the nanoantenna.

At the scattering peak, the coupling of plasmons with emitters can generate emission enhancement due to their high field intensity. The photoluminescence of the emitters also depends on their excitation as they need to absorb a sufficient amount of energy to get their ground state electrons to the excited state.

2.3 Spontaneous emission

Spontaneous emission is defined as a process in which photons are emitted from a quantum system as it converts from an excited state to a ground state. Different molecules, quantum dots (QDs) and semi-conductor quantum wells are typically used as sources of spontaneous emission, however their emission rates are relatively low and are limited by their small physical size and the low photonic density of states of free space. For photonic devices that are based on light emission, a large emission rate is essential for obtaining high-speed devices.

The spontaneous emission sources used in this work are LDS750 fluorescent dyes whose emission peak is around 650 nm. To enhance the spontaneous emission of these dyes, one would have to increase the photonic density of states and change the photonic environment of the emitter. Plasmonic nanostructures are explored for achieving this goal as they support a strongly modified photonic density of states and strong field enhancements, therefore providing flexible means of controlling the spontaneous emission rate of emitters and other light–matter interactions at the nanoscale [15]. The coupling is enhanced between the emitter and the plasmonic resonant mode due to the subwavelength mode volumes of the plasmonic nanostructures. The factor that describes the spontaneous emission rate enhancement is the Purcell factor.

Purcell factor is the modification in the spontaneous emission of a system by its surrounding environment. Purcell's studies established that the coupling between an electric dipole and a resonant cavity results in an enhancement of the decay rate of said dipole in comparison to its free-space decay rate. Therefore, the Purcell Factor is defined as the ratio of the decay rate of the emitter placed in proximity to a resonant cavity, and the one located in free space. In a lossless electromagnetic environment, the Purcell factor describes the change of the total radiated power of an emitter.

$$F = \frac{\gamma}{\gamma_0} = \frac{P_{rad}}{P_{0,rad}}$$

Here γ is the decay rate of the emitter placed in proximity to a resonant cavity, γ_0 is the free-space decay rate, P_{rad} is the total radiated power of the emitter and $P_{0,rad}$ is the corresponding power radiated from the same emitter in free space. It should be noted that this equation ignores the non-radiative losses inside the emitter as this assumption

is applicable to many emitters such as fluorescence dyes and quantum dots [16].

The hyperbolic dispersion of HMMs exhibits modifications in the LDOS around and inside them [7]. This makes the emitters placed on top and inside of HMMs have a wideband enhancement of the emission. The enhancement near the HMMs of the Purcell factor was experimentally shown to reach values of 100 to 10000 for emitters placed inside the HMM [3]. However, the coupling of emitters to bulk HMMs makes the energy from electromagnetic radiation convert to heat as a result of the ohmic losses in the metallic layers [17] resulting in a low enhancement of the far-field radiation.

A recent paper [2] has demonstrated emission enhancement of quantum emitters in the far-field radiation by coupling them to HMM nanocavities which are esentially plasmonic nanoantennas made from HMMs. This work focuses on similar structures however it also explores the effect of the spectral separation of absorption and scattering on the far-field radiation enhancement.

3 METHODS

The following chapter describes experimental and numerical methods that were used to analyse the coupling of the nanoantennas with the fluorescent dye emitters. Previous works have shown that the properties of the nanoantennas are affected by their dimensions. Consequently, this work investigates these properties for different diameters and periods of the nanoantennas. These parameters are chosen with the help of numerical simulations to optimize the resonance wavelengths. Based on the simulation results, the nanoantennas are fabricated using the devices described in this chapter. Finally the last two subsections describe the characterization tools used in this work.

3.1 Simulation

Finite difference time domain (FDTD) solutions of Maxwell's full-wave equations are used to choose the parameters of the nanoantennas. This FDTD method determines the coupling of the incident wave propagating within the nanostructure [18]. This numerical method works by processing small parts of the propagating wave within the nanostructure, that interacts with the wavefront at a given time instant.

The FDTD method uses a Cartesian style mesh, as shown in Figure 3.1, and the direct solutions of Maxwell's curl equations are obtained for each of these mesh points. Consequently, a smaller mesh will result in a more accurate analysis of the structure, but will also require more time and processing memory.

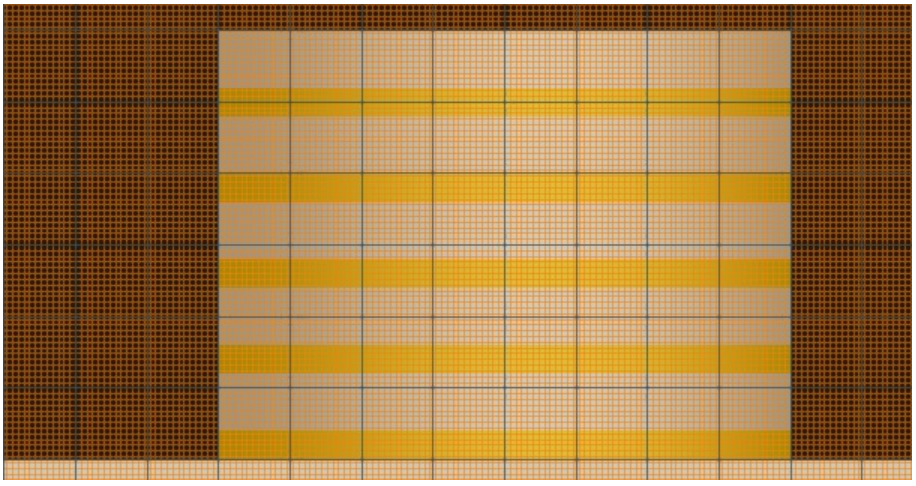

Figure 3.1. *FDTD simulation of a nanoantenna showing each mesh rectangle*

The software Lumerical FDTD Solutions^{TM} is used in this work to identify the initial parameters for the fabrication process and obtain the reflectance, transmittance, scattering and absorption of the nanoantenna structures. The light source used in the simulation resembles a white lamp source. The monitors collect the intensity of each parameter in the range of 450 nm to 950 nm. The boundary conditions for the scattering and absorption simulations are Perfectly Matched Layer (PML) in all the axes. These boundaries act as an absorption layer of the electromagnetic waves incident upon them. The boundary conditions used for reflection and transmission were periodic ones in the x and y axis with periods ranging from 360 nm to 440 nm and PML in the z axis.

The simulations are sometimes different from the experimental results because of factors the software does not take into account like uneven or rough surfaces, etching imperfections etc.

3.2 Fabrication

This subsection covers the fabrication process of the nanoantennas and briefly explains the functionality of the devices used.

First, 10 alternating layers of Ag and SiO_2 are deposited on a fused silica glass sample. The metal and dielectric layers were deposited using E-beam evaporator. During each layer deposition, the original sample is inserted into the device along with a new measuring sample. These measuring samples are later used to measure the thickness of each layer on the original samples since the deposition was done at the same time. A profilometer is used for measuring each metal layer thickness and an elipsometer for measuring the dielectric layers. A basic sketch of one obtained nanoantenna is represented in Figure 3.2

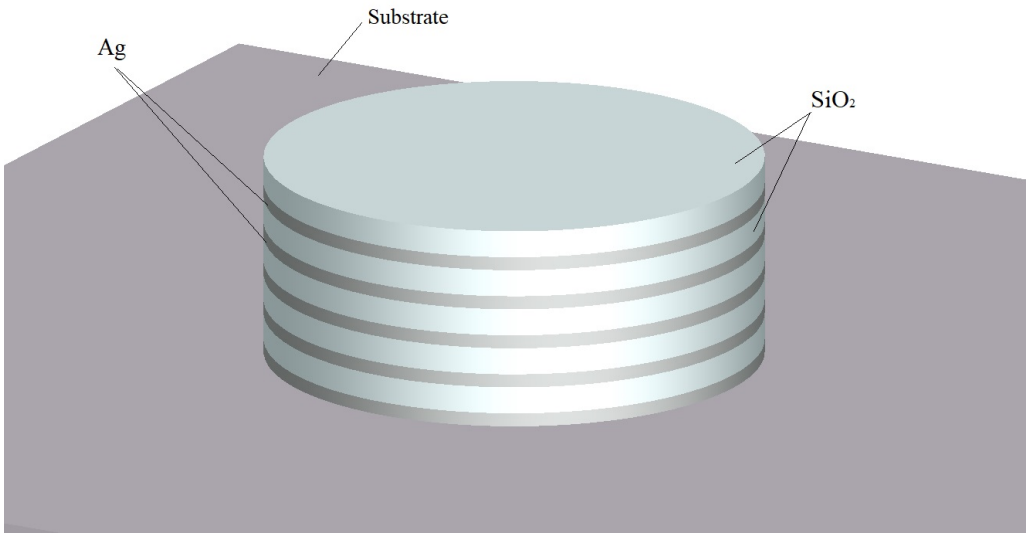

Figure 3.2. *Basic sketch of one nanoantenna*

After the last deposition, a 10 alternating layer Ag/SiO_2 HMM is obtained. In the next step,

a polymer resist is spin-coated on the HMM followed by the E-beam lithography which writes the resist according to the desired parameters. Next, a layer of Ni is deposited on the structure and then a lift-off process is performed with a S1165 remover. The lift-off creates the nano disk of Ni that is used as mask to obtain hyperbolic meta-atoms. The final step is the etching which is performed by a Reactive Ion Etcher. This process involves removing the part of the HMM that is not covered by the Ni while also removing the Ni. This is possible because the etching rate of the Ni is lower than that of the HMM.

The last subsection of this chapter briefly explains the functionality of a scanning electron microscope which is used to obtain an actual image of the fabricated nanoantennas.

3.2.1 E-beam evaporator

E-beam evaporation is a physical vapour deposition technique in which a material is heated by an electron gun in high vacuum, which causes it to evaporate on the desired substrate. The device is made from two chambers, with one on top of the other. A basic sketch of the device is represented by the below Figure 3.3.

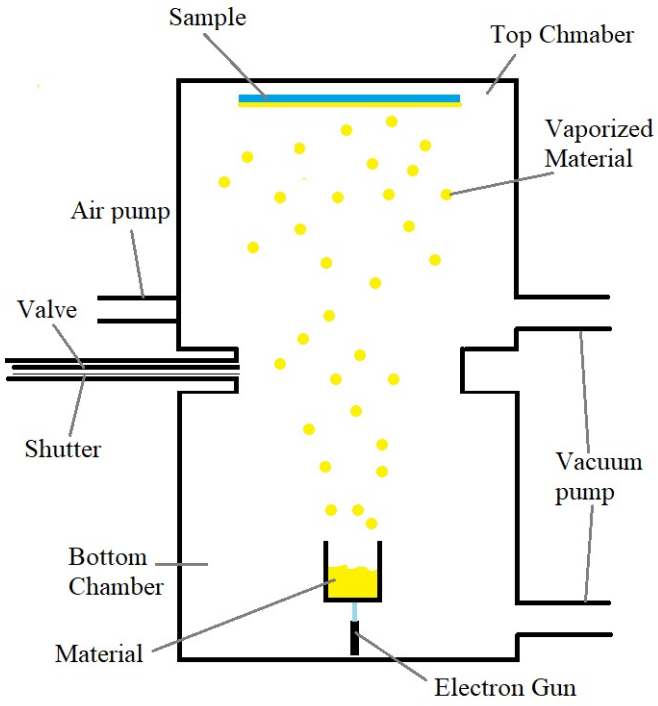

Figure 3.3. *Basic sketch of an E-beam evaporator*

The initial step of the deposition is closing the valve between the two chambers. This is followed by breaking the vacuum on the top chamber and inserting the samples in it. Next, the top chamber is closed and vacuum is applied to it. After the pressure in the top chamber stabilises, the valve opens again automatically. Next comes the heating of the material from the bottom chamber with an electron gun. This is done by applying a voltage and slowly increasing the intensity of the current. As the current increases, so

does the deposition rate and when the required rate is achieved (usually around 0.02 - 0.04 nm/s) the shutter between the two chambers is fully opened and the deposition begins. After the deposition is done, the valve is closed, which is again followed by breaking the vacuum on the top chamber and extracting the samples.

It should be noted that two E-beam evaporators were used for this work. One containing metals and the other containing dielectric materials. In the Dielectric E-beam evaporator another step is required. This step involves heating and maintaining the samples to 100°C after the pressure in the top chamber stabilises. This ensures the adhesion between the sample and the dielectric material that is later evaporated.

Each layer deposition is done separately with two samples: the original sample and a measuring sample. The measuring samples are used to measure the thickness of each layer with a profilometer (for metal layers) and an ellipsometer (for dielectric layers). These devices a covered in the next sections.

3.2.2 Ellipsometer

During the deposition each dielectric layer, the original sample is inserted into the E-beam evaporator along with a new clean sample. The thickness of the dielectric layer on the clean samples is then measured with the ellipsometer. Since the deposition on the clean and original sample was done at the same time, the deposited layer thickness is the same on both. This allows one to estimate the thickness of each dielectric layer on the original sample.

The ellipsometer is a device that measures the thickness and refractive index of a dielectric layer on a substrate. The device's functionality is based on the phase difference between the rays reflected from the dielectric layer and the rays which are transmitted through it and then reflected by the substrate. The ellipsometer can have a measuring range from 1 nm to several microns.

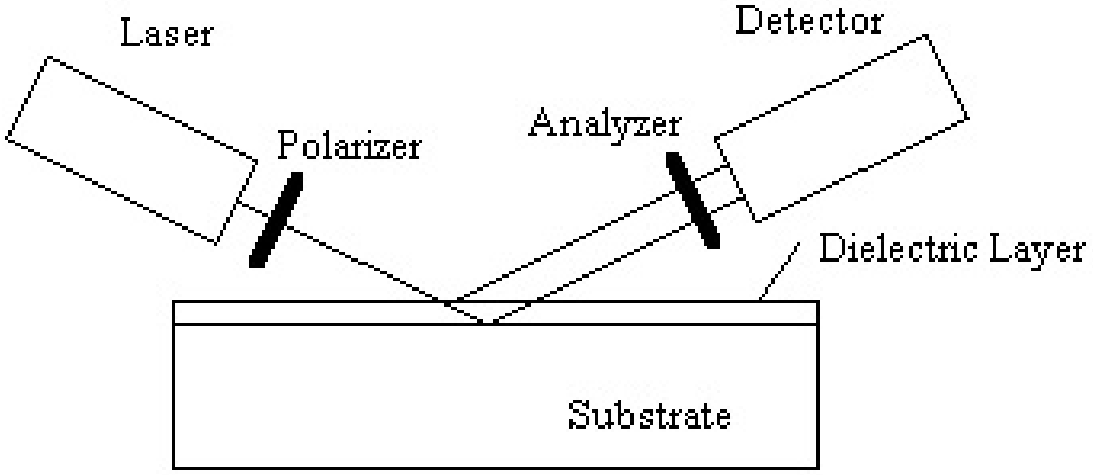

Figure 3.4. *Basic sketch of an ellipsometer [19]*

The device is made out of two sections, separated by the sample. The elements located before the sample produce a known polarization state for the ray that interacts with the sample. When the polarized ray interacts with the sample, it produces a change to the initial polarization. The change in polarization is then determined by the detector. The detector to converts the electromagnetic field into a voltage or current that scales with the irradiance (intensity) of light.

3.2.3 Profilometer

Again, during the deposition each metal layer, the original sample is inserted into the E-beam evaporator along with a new clean sample. The thickness of the metal layer on the clean samples is then measured with the profilometer. Since the deposition on the clean and original sample was done at the same time, the deposited layer thickness is the same on both. This allows one to estimate the thickness of each metal layer on the original sample.

Profilometry is a technique used to extract data from a surface. In this work, the profilometer is used to measure the step height of a metal layer. During the metal deposition, the samples are fixed on the sample holder with a clip, so there is always a part of the sample that does not have any material deposited on it. This is why the profilometer can be used to determine the step height. A representation of the functionality of the profilometer is shown in Figure 3.5.

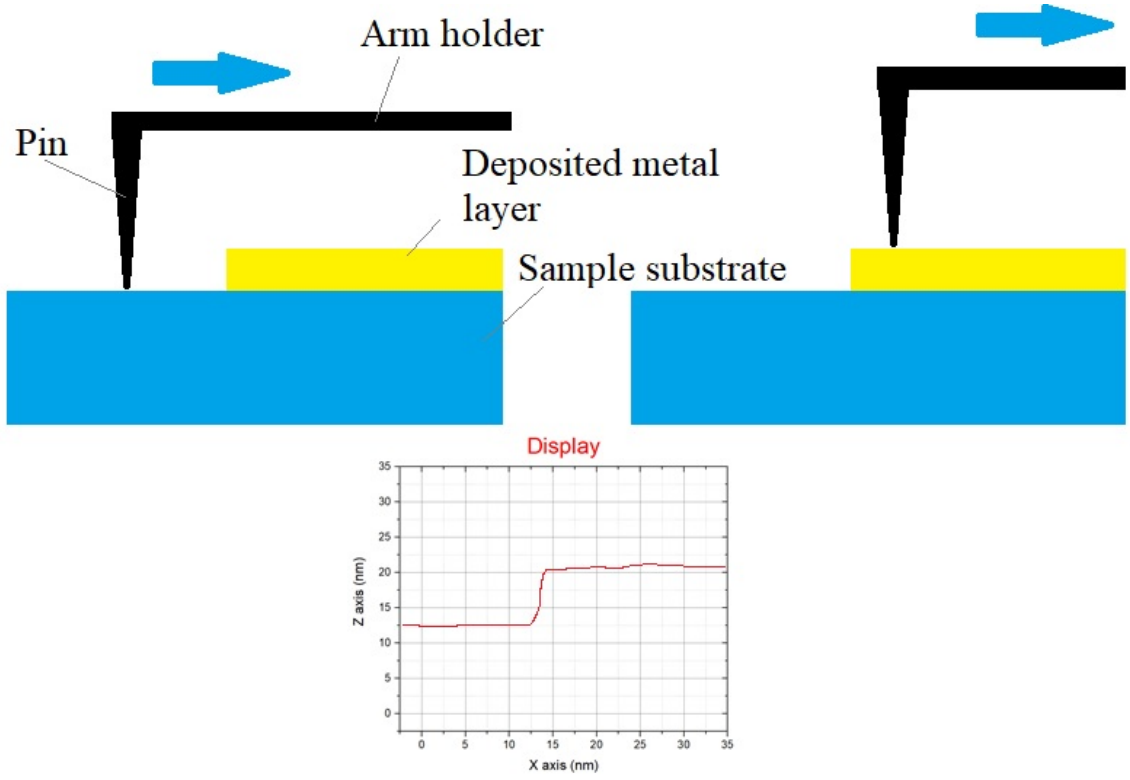

Figure 3.5. *Basic sketch of a profilometer*

The profilometer is made out of a sample stage and a small pin. The sample is placed on the stage and a pin is moved along its surface. This is done by using a feedback loop that measures the force pushing up against the pin as it scans through the sample. A feedback system is used to keep the arm holding the pin at a set-point value of torque. The changes in the position of the arm holder are then be used to digitally reconstruct the structure of the surface.

3.2.4 Spin coating

Spin coating is a fabrication technique that produces a thin, uniform polymer film on a planar surface. This process works by depositing a few drops of a resist solution on a sample and then accelerating the sample with a desired rotational frequency. The resist spreads out radially because of the centrifugal force and the excess is expelled from the edge of the sample. The film continues to become thinner until it reaches an equilibrium thickness or until it solidifies due to an increase of viscosity from the evaporation of the solvent [20]. Figure 3.6 represents the basic functionality of a spin coater.

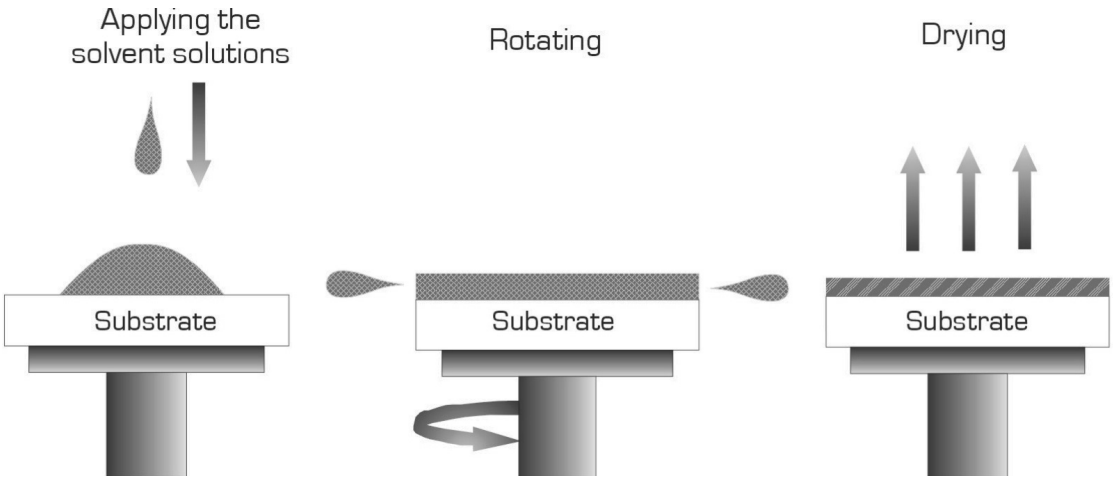

Figure 3.6. *Basic functionality of a spin coater [20]*

In this work, a PMMA A4 950 resist solution is spin coated on the HMM sample with 3000 revolutions per minute for 40 seconds and baked in 180°C, to have a resist layer whose thickness is about 200 nm, which is later used for E-beam lithography.

3.2.5 E-beam lithography

Electron beam lithography is a fabrication technique used to create patterns on a nanoscale. The device is made out of an electron gun, a chamber, and a column. The column and the chamber are always maintained in a high vacuum. The column contains all the elements that create an electron beam, accelerate it to the working voltage, focus it, and deflect it [21]. A visual representation of the device is shown in Figure 3.7.

The device works by focusing an electron beam across a sample covered by an electron-

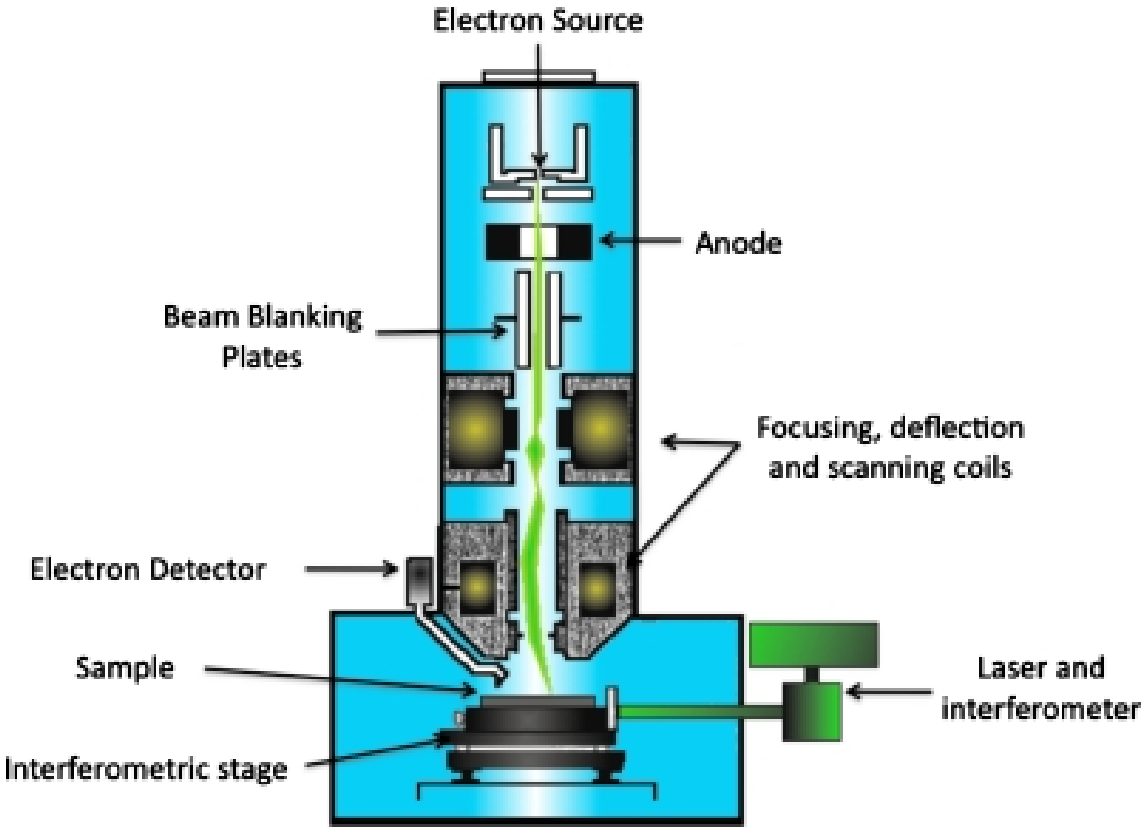

Figure 3.7. *A visual representation of an E-beam lithography device [21]*

sensitive resist that changes its solubility based on the energy delivered by the beam. This causes the exposed areas to be removed.

In this work, the result obtained after the E-beam lithography is a periodic array of holes on the resist. A layer of Ni is then deposited on the sample and then a lift off process with a S1165 remover is performed. The end result after these processes is a HMM sample with a periodic array of Ni disks on top of it.

3.2.6 Reactive ion etcher

The Reactive ion etcher (RIE) is a device that uses chemically reactive plasma to remove the material deposited on samples. The plasma is formed by applying radio frequency power to a cathode, while the anode is grounded. The electric field ionizes the gas molecules, creating plasma. Then, a DC voltage forms on the bottom of the anode and energizes the ions from the plasma. The electrons are then accelerated up and down in the chamber. The electrons deposited on the sample plate make it to build up a large negative charge while plasma itself develops a slightly positive charge due to the higher concentration of positive ions.

This voltage difference causes the positive ions drift towards the sample, where they collide with it. The ions transfer some of their kinetic energy to the sample and consequently start sputtering the material on the surface of the sample. A visual representation of the

RIE is shown in figure 3.8.

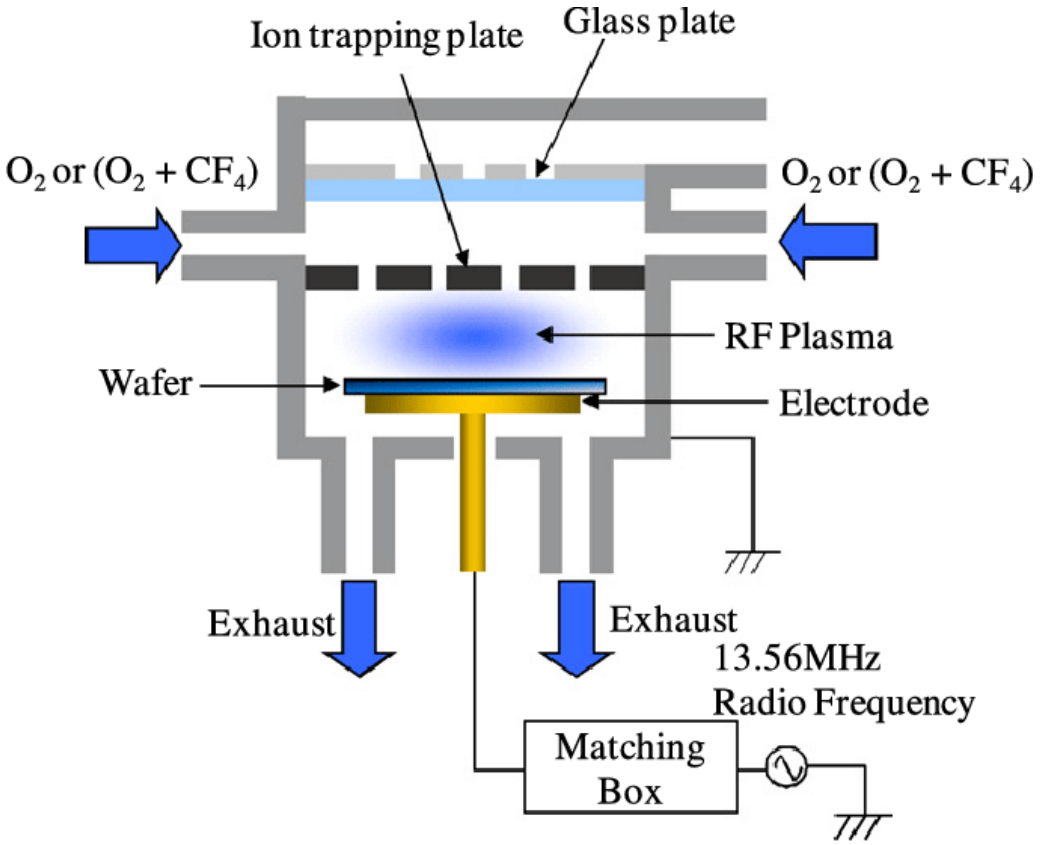

Figure 3.8. *A visual representation of the RIE [22]*

A RIE device is built around a vacuum chamber with two electrodes. Before the chamber is placed under vacuum, the sample is placed on the bottom electrode. Process gases enter the chamber through the showerhead in the top electrode, and the reactor is evacuated by a vacuum pump.

3.3 Characterization

3.3.1 Scanning electron microscope

A Scanning electron microscope (SEM) works by accelerating electrons towards the sample that is to be imaged. Some of these electrons include secondary electrons and back-scattered electrons. These electrons are the ones that produce the SEM images. To be more precise the secondary electrons show the morphology and topography of the samples and the back-scattered electrons illustrate the contrasts. These electrons are collected by a detector and then the signal is converted into an point on the image. These points form based on the electron signal intensity that is detected from the corresponding points on the sample and shown on a screen. This method can provide a high resolution image (less than 1 nm) of the sample surface. A schematic diagram of the SEM working principle is shown in Figure 3.9.

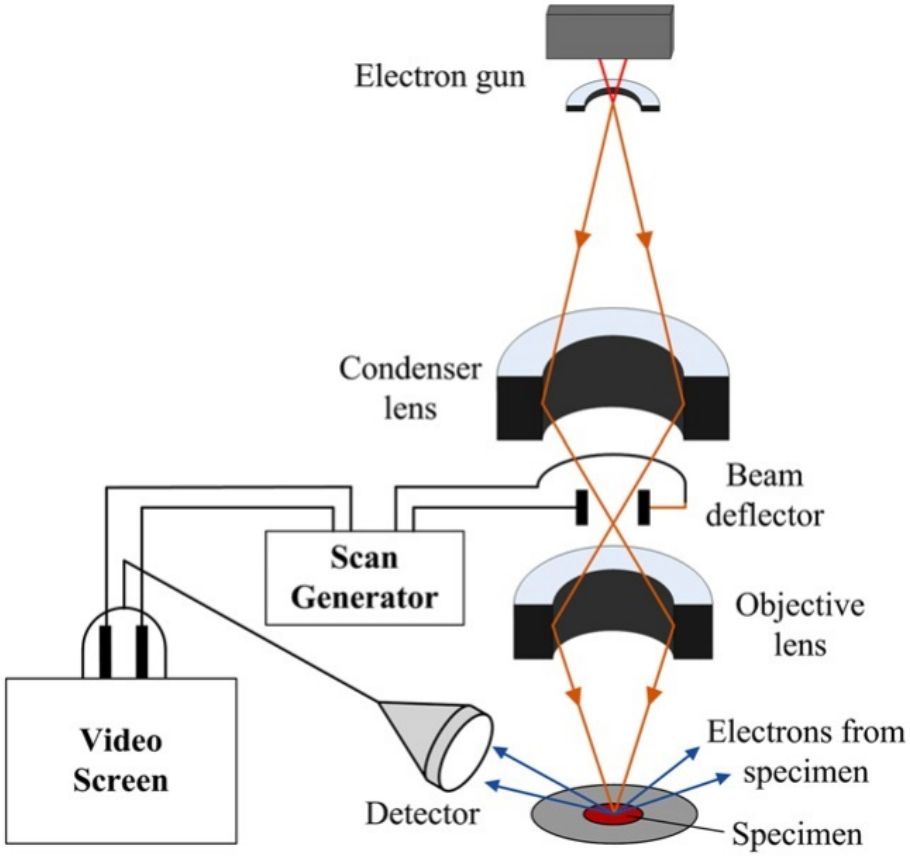

Figure 3.9. *A schematic diagram of the SEM working principle [23]*

In this work the SEM is used to get an image of the fabricated nanoantennas and to measure their period and diameter.

3.3.2 Spectroscopic measurements

The spectroscopic characterization of the nanoantennas is done using on reflection and transmission measurements. The device used for the sample characterization is a confocal microscope (WiTec - alpha 300 series) whose detector operates in the visible spectrum and can be configured to measure reflection, transmission, photo-luminescence etc. A schematic diagram of the microscope is shown in Figure 3.10.

A white light source is used to measure the transmission and reflection. In the reflection measurement, an Al reflector is taken as a reference. This is used by the software to give the correct reflection graph of the sample. After this calculation, the reflection of the nanoantennas is measured. In the transmission measurement, a glass sample is taken as a reference. This glass sample is exactly the same as the substrate of the nanoantenna sample. Then, similar to the reflection measurements, the software colects the background from bare glass and the transmission of the nanoantennas is then measured.

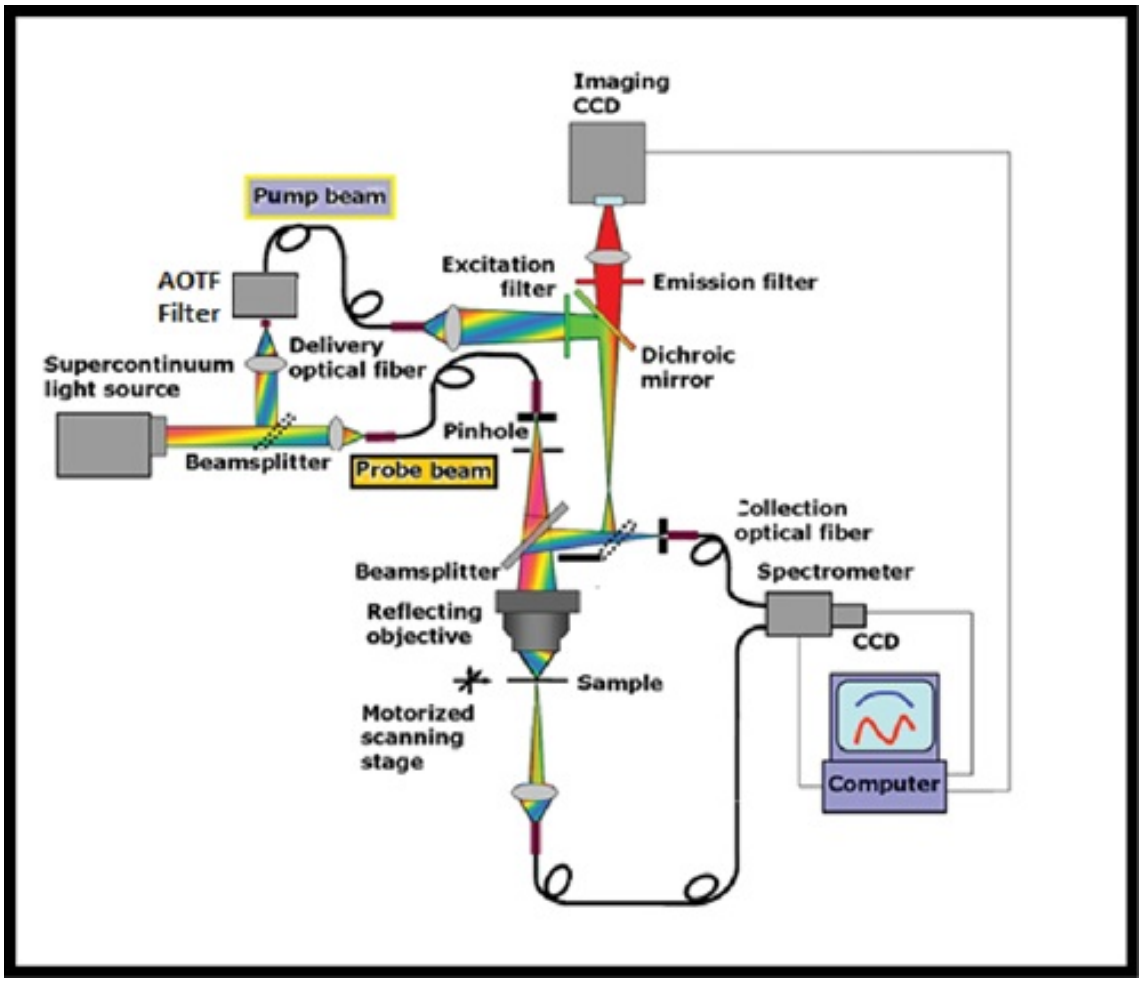

Figure 3.10. *A schematic diagram of the spectroscopy setup in Metaplasmonics Lab.*

3.3.3 Photoluminescence measurements

Firstly, it should be noted that after all the fabrication processes are done and the spectroscopic measurements are taken, a resist solution with LDS750 dyes is spin coated on the sample. Without this, the photoluminescence measurements are not possible since the emission comes from the dye and the nanoantennas are there to enhance it.

The photoluminescence or spontaneous emission measurements are also done with the WiTec confocal microscope, which is represented in Figure 3.10. The microscope can be configured to also perform this task and the configuration is quite similar to the one used to measure reflection as both measurements can be done at the same time. The main difference is that for photoluminescence, 532 nm wavelength continuous wave laser is used as the light source and a 535 nm notch filter is used to stop the reflected excitation wavelength from the sample as the detector would have recognized it as emission which would lead to erroneous results.

4 RESULTS

This chapter covers the results obtained in this work. The first subsection shows the obtained SEM images of the nanoantennas from the top. The next subsection covers the Absorption and scattering FDTD simulations for the Ag-SiO_2 meta-antennas and Ag nanoantennas. The next subsection covers the spectral characterization of the nanoantennas with reflection and transmission experiments. The final subsection covers the photoluminescence measurements.

4.1 Characterization with SEM

After the fabrication of a few HMM samples, one of these samples was turned into a nanoantenna sample through E-beam lithography and RIE. This sample has 18 matrices with nanoantennas that have different diameters and periods. After taking SEM images it was concluded that the periods are 360 nm, 400 nm and 440 nm and the diameters range from 120 nm to 210 nm. Some SEM images of the obtained nanoantennas are represented in Figure 4.1.

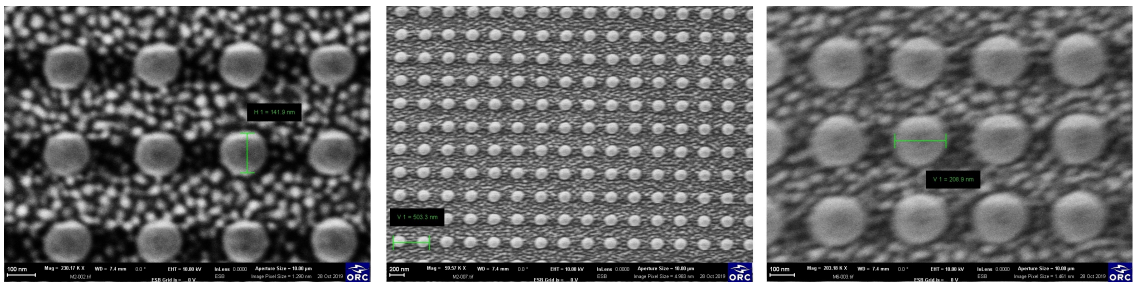

Figure 4.1. *SEM images of nanoantennas with period 360 nm.*

The SEM images were taken for the purpose of having a confirmation that the E-beam lithography and RIE process went well and the obtained structure matches the one desired. As Figure 4.1 shows, the result is a periodic array of nanocylinders which is exactly what was desired.

4.2 Absorption and scattering FDTD simulations

As mentioned earlier, the scattering and absorption peaks overlap for the metal nanoantenna case, while adding dielectric layers between the layers of Ag results in a spectral distribution of the scattering and absorption [5]. This will allow the coupling of the

nanoantennas with the fluorescent dyes that have an emission peak overlapping with the scattering peak of the nanoantennas. Consequently, this coupling should lead to the enhancement of the spontaneous emission.

The absorption and scattering FDTD simulations are represented in figure 4.2. The left graph is for only the Ag nanoantenna case and the right one is for the Ag-SiO_2 hyperbolic metamaterial nanoantenna (meta-antenna).

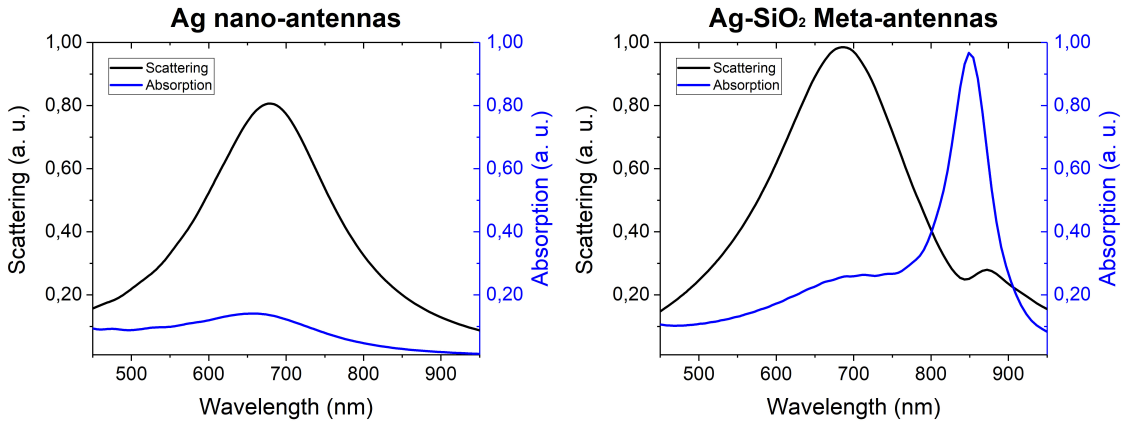

Figure 4.2. *Absorption and scattering FDTD simulation results for a Ag nanoantenna (left) and a Ag-SiO_2 nanoantenna (right)*

The units for absorption and scattering are arbitrary so the graph was normalized. As shown in the figure, the scattering peak is around 690 nm so the emission of the dye should have its peak around that value.

4.3 Spectral characterization of the nanoantennas

The spectroscopic characterization of the nanoantennas is done using the reflection and transmission of the sample. Measuring the scattering would require an integrated sphere setup which is not feasible when considering small spots on a 1cm-by-1cm glass sample. From a physical point of view, reflection and scattering are similar phenomena and the wavelength range with high reflection should also have high scattering. Therefore, the reflection peak can now be used to match the emission peak of the dye.

The reflection and transmission results of nanoantenna samples with period 360 nm are represented in Figure 4.3.

The overall reflection of the nanoantennas was proven to have a low intensity. Some reasons for that might be imperfections in the fabrication or insufficient metal filling factor. According to FDTD simulations, the reflection should have been higher but, as stated before, often times the simulation and experimental results seem to diverge when the structures become very small.

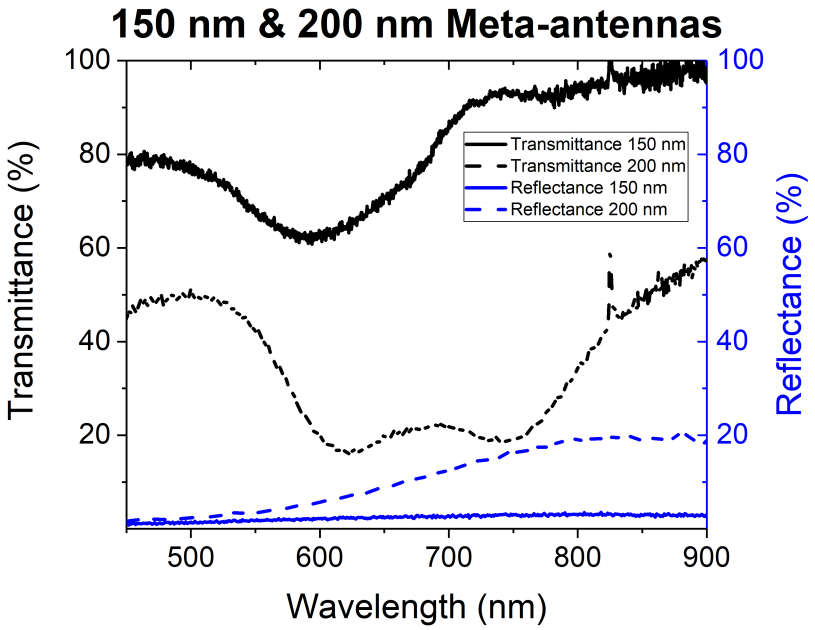

Figure 4.3. *Reflectance and transmittance of nanoantennas with period 360 nm and approximate diameters of 150 nm and 200 nm.*

4.4 Photoluminescence results

As mentioned before, the photoluminescence measurements or the spontaneous emission measurements are performed also with the WiTec confocal microscope but this time using a 532 nm continuouswave laser. The results are shown in Figure 4.4

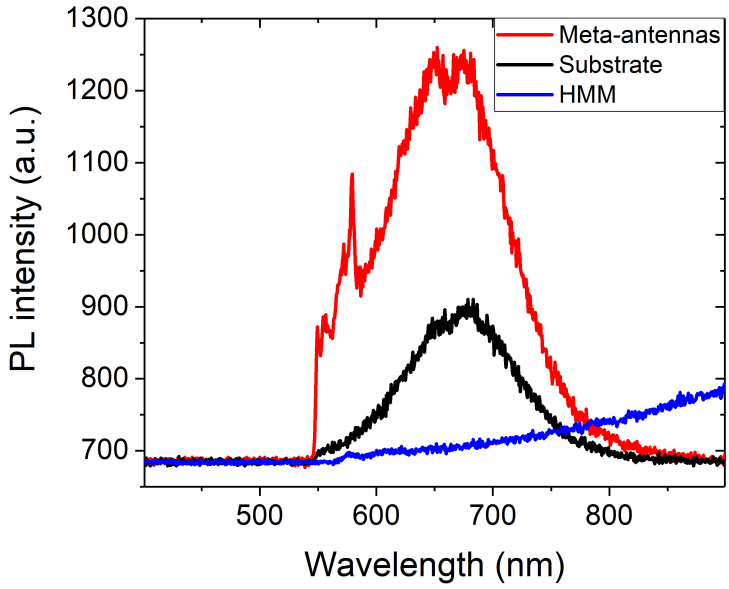

Figure 4.4. *Photoluminescence measurements of the dye on substrate, HMM and meta-antennas*

As is shown in the figure the emission has been enhanced about 1.5 times. The reflection

of the nanoantennas was quite low so the emission enhancement was not as high as expected. To solve this problem, one would need to find a way to increase the reflection and shift it's peak around 650 nm (where the dye has it's emission peak). This can probably be done by increasing the filling factor of the metal in the nanoantenna either by increasing it's thickness or it's diameter.

5 CONCLUSION

This thesis explores the usage hyperbolic meta-antennas, as a candidate for achieving the spectral distribution of the scattering and absorption and enhancing the spontaneous emission. It covers the theoretical background of the hyperbolic meta-antennas and spontaneous emission, the fabrication techniques used, the spectral characterization results and the emission results.

The separation of the scattering and absorption spectrum was the main point of interest for this work, as it would have to overlap properly to the emission peak of the dye to enhance the spontaneous emission. On the other hand, in normal metallic materials, the scattering and absorption peaks overlap completely. This phenomena reduces the coupling with the dye and reduces the enhancement of the emission so the separation of scattering and absorption would further increase the spontaneous emission. This is achieved using hyperbolic meta-antennas made from alternating layers of Ag and SiO_2. They were fabricated with different techniques including: metal coating, dielectric coating, lithography, RIE etc. After the fabrication process, the reflection and transmission were measured experimentally and the scattering and absorption was computed using FDTD simulations. After achieving the spectral distribution, the meta-antenna samples were spin-coated with LDS750 dyes and the photo-luminescence measurements were taken resulting in a 1.5 enhancement of the emission.

Overall, this work can be continued to study further light-matter interactions with meta-antennas and the relation between the spectral separation of scattering and absorption and the spontaneous emission enhancement by using more reflective samples, as the reflection intensity of the obtained samples was low. This can be done by increasing the metal filling factor, increasing the periodicity or using a different metal. Initially the metal layer of the meta-antennas were made from Au but their reflection peak seemed to be around 750 nm - 800 nm which does not match the emission peak of the LDS 750 dye. However, this design can also be explored using another dye that emits around the respective wavelength region.

REFERENCES

[1] Shekhar, P., Atkinson, J. and Jacob, Z. Hyperbolic metamaterials: fundamentals and applications. *Nano convergence* 1.1 (2014), 14.

[2] Indukuri, S. C., Bar-David, J., Mazurski, N. and Levy, U. Ultrasmall Mode Volume Hyperbolic Nanocavities for Enhanced Light–Matter Interaction at the Nanoscale. *ACS nano* 13.10 (2019), 11770–11780.

[3] Tumkur, T., Zhu, G., Black, P., Barnakov, Y. A., Bonner, C. and Noginov, M. Control of spontaneous emission in a volume of functionalized hyperbolic metamaterial. *Applied Physics Letters* 99.15 (2011), 151115.

[4] Ferrari, L., Wu, C., Lepage, D., Zhang, X. and Liu, Z. Hyperbolic metamaterials and their applications. *Progress in Quantum Electronics* 40 (2015), 1–40.

[5] Maccaferri, N., Zhao, Y., Isoniemi, T., Iarossi, M., Parracino, A., Strangi, G. and De Angelis, F. Hyperbolic meta-antennas enable full control of scattering and absorption of light. *Nano letters* 19.3 (2019), 1851–1859.

[6] Noginov, M., Li, H., Barnakov, Y. A., Dryden, D., Nataraj, G., Zhu, G., Bonner, C., Mayy, M., Jacob, Z. and Narimanov, E. Controlling spontaneous emission with metamaterials. *Optics letters* 35.11 (2010), 1863–1865.

[7] Jacob, Z., Kim, J.-Y., Naik, G. V., Boltasseva, A., Narimanov, E. E. and Shalaev, V. M. Engineering photonic density of states using metamaterials. *Applied physics B* 100.1 (2010), 215–218.

[8] Yao, J., Liu, Z., Liu, Y., Wang, Y., Sun, C., Bartal, G., Stacy, A. M. and Zhang, X. Optical negative refraction in bulk metamaterials of nanowires. *Science* 321.5891 (2008), 930–930.

[9] Hoffman, A. J., Alekseyev, L., Howard, S. S., Franz, K. J., Wasserman, D., Podolskiy, V. A., Narimanov, E. E., Sivco, D. L. and Gmachl, C. Negative refraction in semiconductor metamaterials. *Nature materials* 6.12 (2007), 946–950.

[10] Liu, Z., Lee, H., Xiong, Y., Sun, C. and Zhang, X. Far-field optical hyperlens magnifying sub-diffraction-limited objects. *science* 315.5819 (2007), 1686–1686.

[11] Yao, J., Yang, X., Yin, X., Bartal, G. and Zhang, X. Three-dimensional nanometer-scale optical cavities of indefinite medium. *Proceedings of the National Academy of Sciences* 108.28 (2011), 11327–11331.

[12] Jacob, Z., Smolyaninov, I. I. and Narimanov, E. E. Broadband Purcell effect: Radiative decay engineering with metamaterials. *Applied Physics Letters* 100.18 (2012), 181105.

[13] Guo, Y., Cortes, C. L., Molesky, S. and Jacob, Z. Broadband super-Planckian thermal emission from hyperbolic metamaterials. *Applied Physics Letters* 101.13 (2012), 131106.

[14] Giannini, V., Fernandez-Dominguez, A. I., Heck, S. C. and Maier, S. A. Plasmonic nanoantennas: fundamentals and their use in controlling the radiative properties of nanoemitters. *Chemical reviews* 111.6 (2011), 3888–3912.

[15] Hoang, T. B., Akselrod, G. M., Argyropoulos, C., Huang, J., Smith, D. R. and Mikkelsen, M. H. Ultrafast spontaneous emission source using plasmonic nanoantennas. *Nature communications* 6.1 (2015), 1–7.

[16] Krasnok, A. E., Slobozhanyuk, A. P., Simovski, C. R., Tretyakov, S. A., Poddubny, A. N., Miroshnichenko, A. E., Kivshar, Y. S. and Belov, P. A. An antenna model for the Purcell effect. *Scientific reports* 5 (2015), 12956.

[17] Guo, Y., Newman, W., Cortes, C. L. and Jacob, Z. Applications of hyperbolic metamaterial substrates. *Advances in OptoElectronics* 2012 (2012).

[18] Taflove, A. Application of the finite-difference time-domain method to sinusoidal steady-state electromagnetic-penetration problems. *IEEE Transactions on electromagnetic compatibility* 3 (1980), 191–202.

[19] Zeghbroeckn, B. V. The ellipsometer. (1997).

[20] Dobrzański, L. and Szindler, M. Sol gel TiO2antireflection coatings for Silicon solar cells. *Journal of Achievements in Materials and Manufacturing Engineering* 52.1 (2012), 7–14.

[21] Altissimo, M. E-beam lithography for micro-/nanofabrication. *Biomicrofluidics* 4.2 (2010), 026503.

[22] Wang, C. and Suga, T. Investigation of fluorine containing plasma activation for room-temperature bonding of Si-based materials. *Microelectronics Reliability* 52.2 (2012), 347–351.

[23] Zhu, F.-Y., Wang, Q.-Q., Zhang, X.-S., Hu, W., Zhao, X. and Zhang, H.-X. 3D nanostructure reconstruction based on the SEM imaging principle, and applications. *Nanotechnology* 25.18 (2014), 185705.